Journal of Applied Polymer Science

Evolution of Mechanical Properties During Cure for Out-of-Autoclave Carbon-Epoxy Prepregs

Khalil Vora, Tien Vo, Mohammad Islam, Mohammad Habibi, Bob Minaie
Department of Mechanical and Aerospace Engineering, California State University, Long Beach, California 90840
Correspondence to: B. Minaie (E-mail: Bob.Minaie@CSULB.edu)

ABSTRACT: Extent of cure and rheological properties were obtained for out-of-autoclave materials, Cycom 5320-8HS and Cycom 5320-PW, for the manufacturer recommended cure cycle using differential scanning calorimeter and encapsulated sample rheometer (ESR), respectively. Rheological properties from ESR were further used in designing the cure cycles to study the evolution of mechanical properties. Five panels were cured at different cure stages using the designed cure cycles and coupons were tested for short beam shear and combined loading compression properties at different cure stages. To correlate the mechanical properties with its respective glass transition temperature, dynamic mechanical analyzer was used to obtain the glass transition temperature for the coupons obtained from the respective panels. Statistical results showed significant difference in short beam shear and combined loading compression properties up to vitrification, however, no significant difference was observed on these mechanical properties after vitrification. The observed linear trend between degree of cure (DOC) and glass transition temperature (T_g) was validated using DiBenedetto relation. Linearly increasing trend between DOC and glass transition temperature (T_g) for different cure states suggests that both DOC and T_g can be used interchangeably to define the state of material. A good correlation was observed between material cure state and the mechanical properties. A mathematical model was also proposed to determine the short beam shear and combined loading compression properties based on material cure state. © 2014 Wiley Periodicals, Inc. J. Appl. Polym. Sci. **2015**, *132*, 41548.

KEYWORDS: differential scanning calorimetry; glass transition; mechanical properties

Received 12 April 2014; accepted 22 September 2014
DOI: 10.1002/app.41548

INTRODUCTION

Recent developments in out-of-autoclave technology have lead to a point where the autoclave quality parts are achievable with a consolidation absolute pressure of 1 atmosphere only.[1] Beside the energy savings, these low pressure cured parts eliminate expensive tooling and equipment costs associated with autoclave manufacturing. Moreover, the size of the autoclave limits the cured part size and thus imposes tedious assembly requirements. Unlike autoclave prepreg, out-of-autoclave materials are usually semi-impregnated to provide low porosity even under a low pressure application. For out-of-autoclave prepregs, porous regions during manufacturing are created by applying the resin to the outer surface of prepregs to remove entrapped air within the uncured laminate stack and to provide enough consolidation pressure for the resin to flow into the dry regions during the elevated temperature.[1] During the cure, viscosity of the resin should be low enough and to be maintained for a sufficient period of time to completely wet the fibers and hence eliminating the possibility of voids locked in. As a general rule, higher initial temperature will lead to lower initial resin viscosity. However, with the elevated initial temperature the resin may start to gel sooner and hence will not provide sufficient time to remove the entrapped air. Therefore, knowledge of cure kinetics[2–7] and rheology[4,7,8] is necessary in designing the cure cycle for a given material. Gillham et al. introduced the concept of time–temperature transformation (TTT) diagram[9] and several studies have been performed since then to model the kinetic and rheological behavior of resin during the cure. These models are helpful in designing the cure cycles and to aid in the process development. While several studies have been performed to model the cure kinetics during prepreg processing, unfortunately, none of the available models can estimate the mechanical properties development during the cure.

Development of mechanical, physical, and thermal properties of an out-of-autoclave prepreg composite is a complex process. Although the prepreg are normally processed using the isothermal curing, the development of its properties are generally nonlinear and hence are difficult to predict. It is known that the mechanical properties are highly dependent on the path of viscoelastic properties during cure. However, only a few observations and correlations have been made to date between viscoelastic and mechanical properties since most of the available

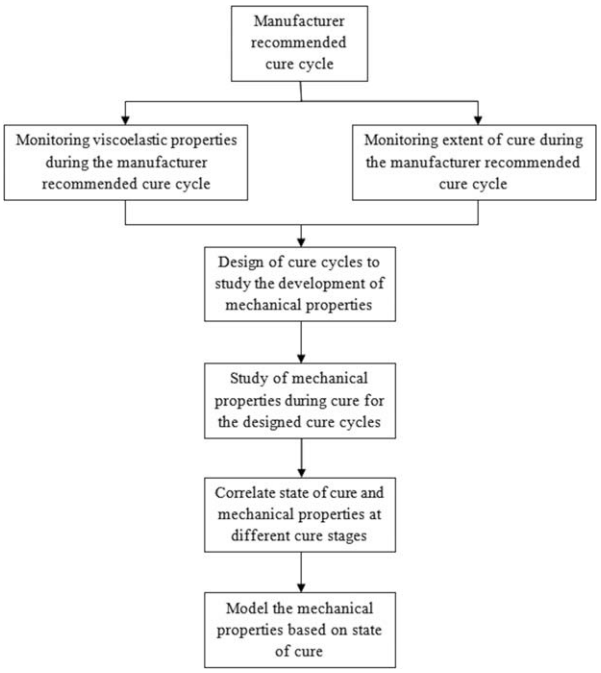

Figure 1. Technical approach for modeling mechanical properties during the cure.

methods of measuring viscoelastic behavior do not produce consistent results and hence the variation in results does not allow the estimation of mechanical properties during the cure.[5] To overcome such problems, an *ex situ* encapsulated sample rheometer (ESR) has demonstrated to be better technique.[10] Unlike other methods, which either depends on sample preparation or may not measure the viscoelastic properties during the whole curing process, this method can monitor the real time viscoelastic properties for the full range of material state, i.e., from low viscosity region to fully cured high rigid state. It is important to know the relationship between state of cure and mechanical properties of composite materials. Mathematical modeling of composite material properties development during and after cure can lead to significant amount of time and money savings. In this work, out-of-autoclave prepregs, Cycom 5320-8HS and Cycom 5320-PW were examined at different stages of manufacturer recommended cure cycle. Figure 1 shows the block diagram of technical approach used for this study.

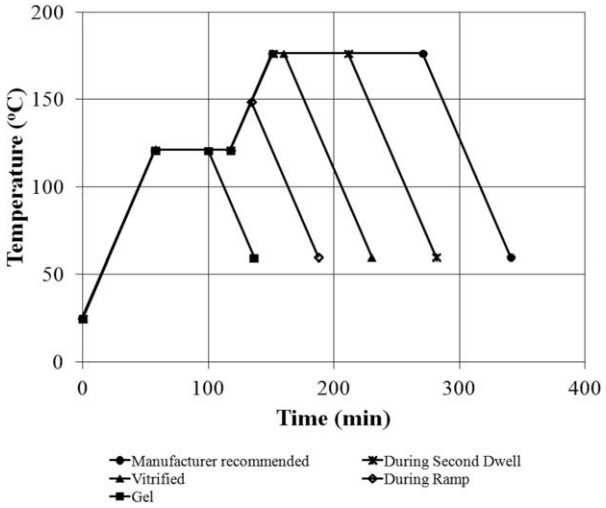

Figure 2. Cure cycles for 5320-8HS and 5320-PW.

EXPERIMENTAL

Material

Two out-of-autoclave materials were investigated in this study having same resin, but different weave system.

5320-8HS. This out-of-autoclave (OOA) toughened epoxy resin, formulated by Cytec, is supplied with 5320 resin system and T650 8-harness satin (8HS) reinforced carbon fibers. This OOA prepreg produces low porosity parts without any external pressure. The manufacturer recommended cure cycle for this prepreg is isothermal cure at 121°C for 60 min followed by freestanding postcure at 177°C for 120 min.

5320-PW. Similar to 5320-8HS, this material also contains 5320 resin system and T650 carbon fibers. The fibers of this prepreg are interlaced to fabricate plain weave fabric. Since this prepreg also contains the same resin system, cure cycle for this prepreg is same as 5320-8HS, i.e., isothermal cure at 121°C for 60 min followed by freestanding postcure at 177°C for 120 min.

Cure Cycles

The manufacturer recommended cure cycle for the material is shown as cure cycle number 5 in Table I. To study the development of cure state during the manufacturer recommended cure cycle, cure cycles 1–4 of Table I were customized from the manufacturer recommended cure cycle using the viscoelastic

Table I. Cure Cycles for 5320-8HS and 5320-PW

Cure cycle no.	First ramp-up (°C/min)	Intermediate cure temp. (°C)	Intermediate cure time (min)	Second ramp-up (°C/min)	Postcure Temp. (°C)	Postcure time (min)
1	1.67	121	42	-	-	-
2	1.67	121	60	1.67	149[a]	[a]
3	1.67	121	60	1.67	177	9
4	1.67	121	60	1.67	177	60
5	1.67	121	60	1.67	177	120

[a] For cure cycle number 2, to obtain properties during the ramp, the curing had been stopped during the second ramp-up at 149°C.

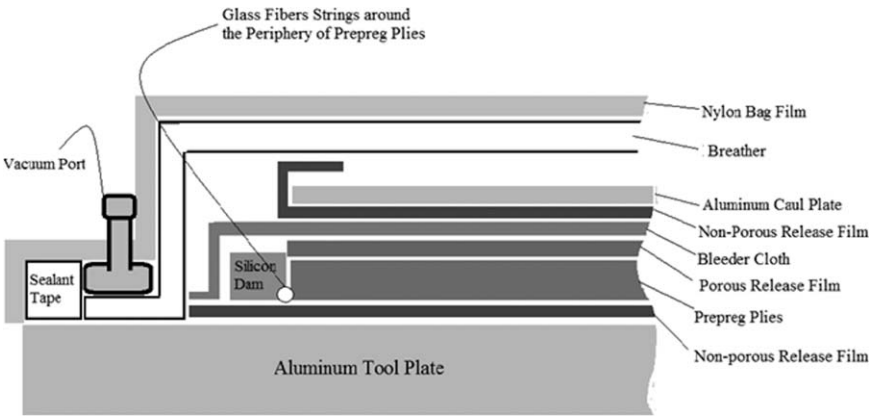

Figure 3. Panel layup schematic for 5320-8HS and 5320-PW panels.

properties and will be discussed in more detail in "Results and Discussion" section.

To eliminate any possible void effects on mechanical properties, variation in cure cycle were introduced after the gel point to keep the minimum viscosity time and gel time constant and hence eliminating any possible porosity level variations between different panels.

Equipments and Testing

Differential Scanning Calorimetry Testing. A differential scanning calorimetry technique was used to study the cure kinetics of 5320-8HS and 5320-PW prepreg materials using a TA Instruments Q2000 differential scanning calorimeter. The prepreg samples of about 10–15 mg in weight were tested in Tzero aluminum pans. The heat of reaction and the degree of cure of the samples were measured for temperature profiles shown in Figure 2. During the cure cycle, the degree of cure (DOC) at time t is given by

$$\alpha(t)=\frac{H(t)}{H_U} \tag{1}$$

where $H(t)$ is the total amount of heat released from the sample up to time 't' during ramp and isothermal cycles and is defined as

$$H(t)=\int_0^t \left(\frac{dQ}{dt}\right) dt \tag{2}$$

H_U, the ultimate heat of reaction, is defined as

$$H_U=H_T+H_{res} \tag{3}$$

where H_T is the total heat released at each combined cure cycle and H_{res} is the residual heat and can be determined by the area under the heat flow curve in dynamic scanning when the exothermic reactions start

$$H_{\text{res}}=\int_{t_s}^{t_e} \left(\frac{dQ}{dt}\right) dt \tag{4}$$

where t_s and t_e represent the start time and the end time of the exothermic reactions during dynamic scanning, respectively.

After substituting eqs. (3) into (1), the degree of cure (DOC) can be written as

$$\alpha(t)=\frac{H(t)}{H_T+H_{\text{res}}} \tag{5}$$

Subsequently, the rate of the degree of cure (DOC) is

$$\frac{d\alpha(t)}{dt}=\frac{dH(t)/dt}{H_T+H_{\text{res}}} \tag{6}$$

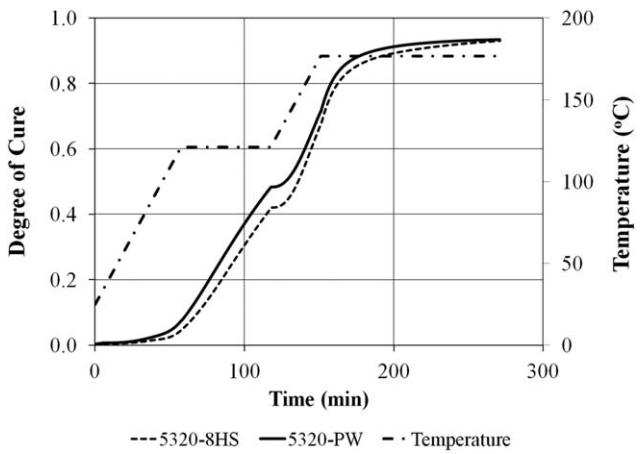

Figure 4. Degree of cure during the manufacturer recommended cure cycle for 5320-8HS and 5320-PW.

Shear Rheometry Testing. Viscoelastic properties of the prepreg during cure are an important parameter that determines the

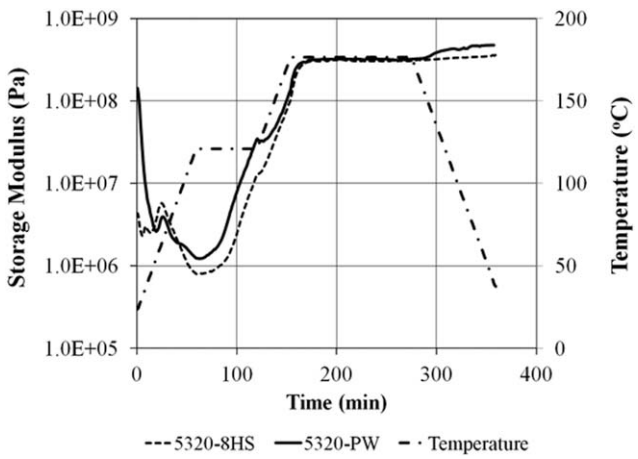

Figure 5. Storage modulus for 5320-8HS and 5320-PW using ESR.

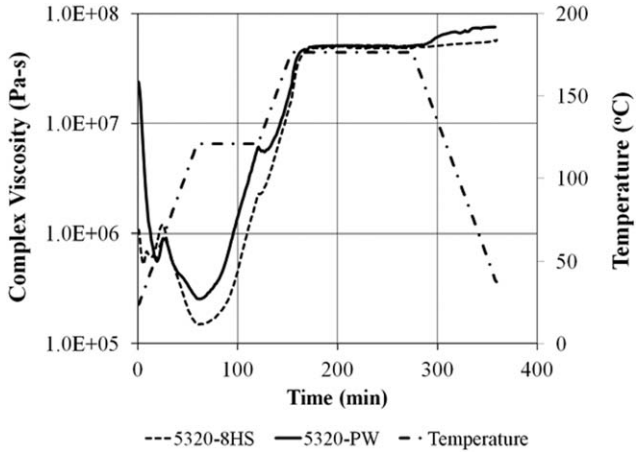

Figure 6. Complex viscosity for 5320-8HS and 5320-PW using ESR.

quality of cured laminate. The acceptable cure zones can then be determined by plotting time–temperature transformation diagram.[11–14] These properties include minimum viscosity, minimum viscosity time, gel time, vitrification time, storage modulus (G'), loss modulus (G''), and tan δ (G''/G'). This approach provides perspicacious view of cure state properties. For instance, a higher absolute value of minimum viscosity value or less time difference between minimum viscosity and gel time may lead to higher porosity level within a cured laminate.

Gel time is a parameter which indicates that the curing material has created a 3-D network of interlinked polymer chains. It is characterized by a rapid increase in viscosity as the mobility of the molecular structure becomes more limited.

Vitrification is the point at which the state of the material changes from the rubber like material to the solid glassy state. At vitrification, the instantaneous glass transition temperature equals the cure temperature and hence the cure reaction transits from kinetic controlled to diffusion controlled mode. After vitrification, the limited mobility of molecules considerably slows down further reactions.[15]

Viscoelastic properties of the samples were obtained using encapsulated shear testing on AvPro ATD CSS 2000 rheometer for prepreg

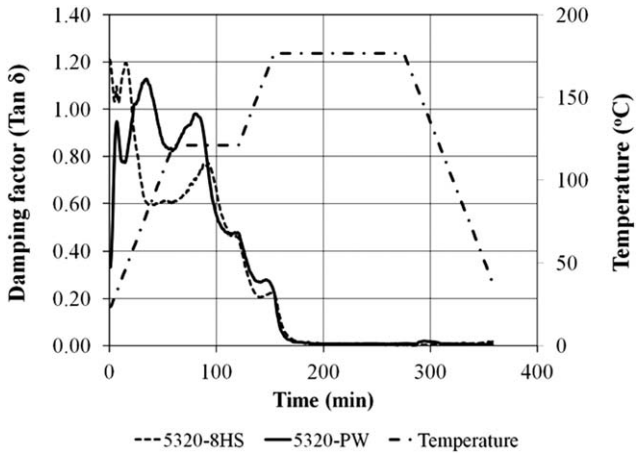

Figure 7. Damping factor (tan δ) during cure for 5320-8HS and 5320-PW using ESR.

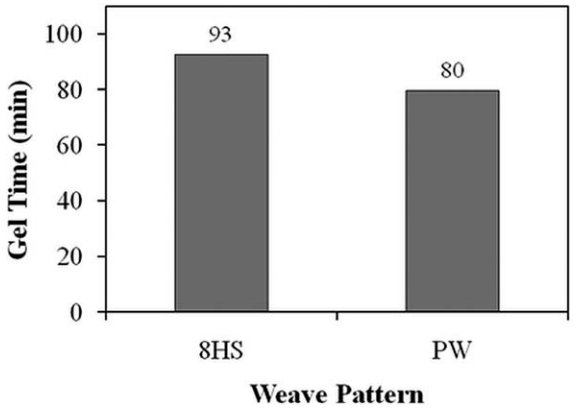

Figure 8. Gel time for 5320-8HS and 5320-PW using ESR.

material. The AvPro ATD CSS 2000 rheometer consists of two parallel plates with 41.3 mm diameter. Each plate is designed with 20 grooves arranged in radial fashion to prevent the sample slippage at high torque. Rheometer samples consisting of 9 plies and 16 plies for 5320-8HS and 5320-PW, respectively, with a nominal cured thickness of 2.8 mm were used in this study. To prevent the bleeding during cure and to ease the removal of sample after testing, all samples were tested with O-ring and Kapton film. Experiments were conducted at a strain of 0.05° and a constant frequency of 1 Hz. To compare the viscoelastic properties with the mechanical properties, rheometer samples were tested using the cure profile number 5 of Table I. This instrument gives real time complex viscosity during the applied temperature cycle which was used to capture important material transitions during the cure.

G' is very similar to the shear modulus (G), but may not have the same value due to its dynamic nature. G'' signifies energy losses due to the heat and viscous effects during the stress/strain cycle. These terms can also be combined to form a complex dynamic modulus G^* as shown in the following equation[16,17]:

$$\frac{G^*}{i\omega} = \left(\frac{G' + iG''}{i\omega}\right) = \eta^* \tag{7}$$

where G^* is the complex dynamic modulus, G' is the storage modulus, G'' is the loss modulus, and η^* is the complex viscosity. These properties are related to tan(δ) by the equation:

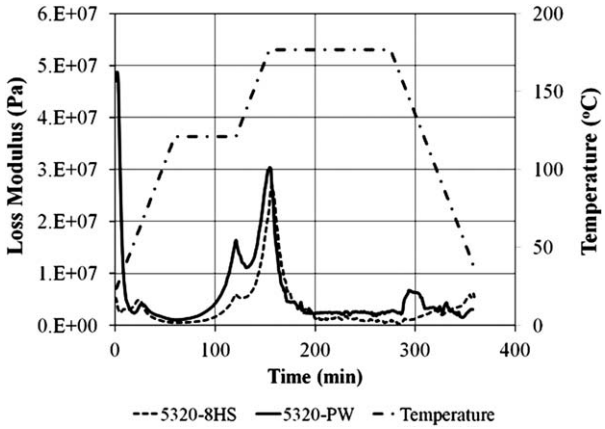

Figure 9. Loss modulus during cure for 5320-8HS and 5320-PW using ESR.

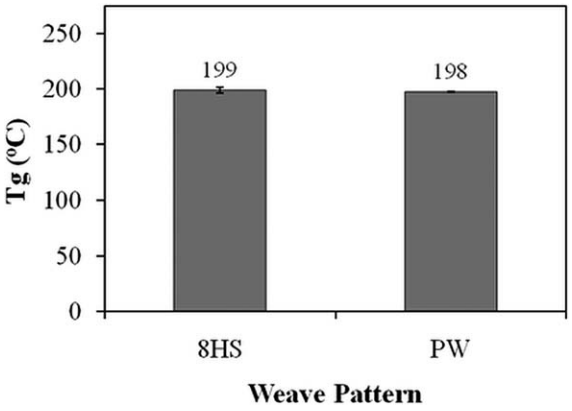

Figure 10. Vitrification time for 5320-8HS and 5320-PW using ESR.

$$\tan(\delta) = \frac{G''}{G'} \quad (8)$$

Glass Transition Temperature (T_g) Testing. Similar to degree of cure, glass transition temperature is an important parameter in defining the state of cure.[18] Since T_g mark a physical change in state of the material, it can be accurately determined by either dynamic mechanical analyzer (DMA) or encapsulated sample rheometer (ESR). In this work, to correlate glass transition temperature with the mechanical properties, DMA was used to determine the T_g using three point bending clamp according to ASTM D7028-07.[19] A heat-up rate of 5°C/min with a frequency of 1 Hz and a strain percentage of 0.02% were used to determine T_g.

Mechanical Testing. For mechanical testing, in order to obtain balanced symmetric laminates, the panel lay-up was 12 plies of prepreg placed in quasi-isotropic sequence order $[0/45]_{3s}$ for 5320-8HS and 24 plies of prepreg placed in quasi-isotropic sequence $[0/45]_{6s}$ for 5320-PW. Figure 3 shows the panel layup schematic for 5320-8HS and 5320-PW panels used in this study. Panels were debulked for 16 h prior to curing. A minimum of 27 in. Hg vacuum was applied throughout the debulking and curing process. To assure the quality of the panels, all the panels were c-scanned before being machined.

Short Beam Shear Testing. The complexity of stresses and the variety of failure modes generally does not allow relating the short beam shear strength to any material property. However, this strength can be used for quality control purposes.[20] For this study, the panels were machined into coupons and five specimens were tested from each panel for their respective short beam shear (SBS) properties according to ASTM standard D2344.

Table II. Average SBS Strength for 5320-8HS and 5320-PW Material for Manufacturer Recommended Cure Cycle

Material	SBS strength (MPa)	Standard deviation (MPa)	Coefficient of variation (CV)
5320-8HS	79.79	5.9	0.07
5320-PW	90.76	1.4	0.02

Combined Loading Compression Testing. Unlike short beam shear strength, combined loading compressive strength is a property that is used for material specifications and design purposes. Combined loading compression (CLC) tests were performed according to ASTM D6641.[21] Three tests coupons were prepared and tested carefully from each panel to prevent premature end crushing and also to prevent excessive induced bending or buckling during the testing.

RESULTS AND DISCUSSION

Final Thermal and Mechanical Properties for Manufacturer Recommended Cure Cycle

Differential Scanning Calorimetry Testing. The instantaneous degree of cure was calculated using eq. (6). Figure 4 shows the development of extent of cure during the manufacturer recommended cure cycle for 5320-8HS and 5320-PW. As shown in Figure 4, significant difference was observed in degree of cure during the curing process and the degree of cure for 5320-PW was observed higher than 5320-8HS during the first dwell temperature. However, this difference was gradually minimized during the second ramp and isothermal soak and finally diminished during the end of curing process. As such, final degree of cure for 5320-8HS and 5320-PW were observed to be around 93%.

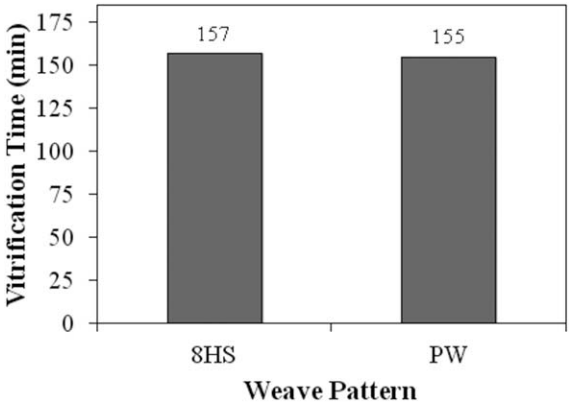

Figure 11. Glass transition temperature for 5320-8HS and 5320-PW for manufacturer recommended cure cycle.

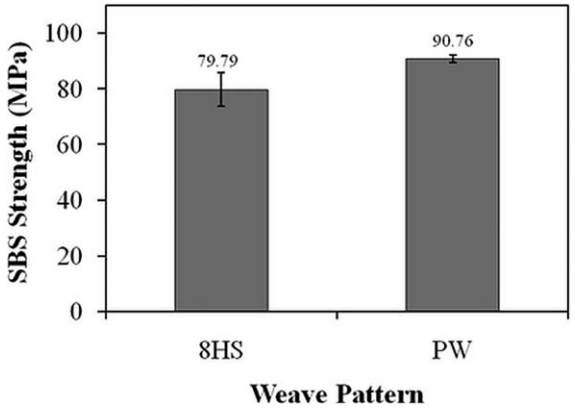

Figure 12. Short beam shear strength for 5320-8HS and 5320-PW for manufacturer recommended cure cycle.

Table III. Two-Sample *t*-Test for SBS Strength Comparison Between 5320-8HS and 5320-PW Panels Cured Using Manufacturer Recommended Cure Cycle

Material	No. of samples	Mean	Std. deviation	Std. error of mean
5320-8HS	5	79.79	5.94	2.70
5320-PW	5	90.76	1.37	0.61

Difference = μ (PW) − μ (8HS).
Estimate for difference: 10.97 MPa.
95% confidence interval difference: 3.40–18.54 MPa.

Table IV. Two-Sample *t*-Test for CLC Strength Comparison Between 5320-8HS and 5320-PW Panels Cured Using Manufacturer Recommended Cure Cycle

Material	No. of samples	Mean	Std. deviation	Std. error of mean
5320-8HS	3	448.0	20.7	12
5320-PW	3	511.0	28.2	16

Difference = μ (PW) − μ (8HS).
Estimate for difference: 63 MPa.
95% confidence interval difference: −1.20 to 127.2 MPa.

Viscoelastic Properties Using Shear Rheometry Testing. Both the in-phase and out-of-phase part of the dynamic modulus, storage, and loss modulus, were obtained by real-time monitoring of the prepreg curing using ESR.

Storage Modulus. Figure 5 shows the storage modulus (G') during cure for 5320-8HS and 5320-PW plotted on a semilog scale, for manufacturer recommended cure cycle. Storage modulus of viscoelastic material estimates the elastic behavior of the material. Initially the heat energy started melting the resin in the prepreg and hence storage modulus started decreasing. Once its minimum value reached, the crosslinking started and the storage modulus started picking up for both the materials. Significant difference was observed in storage modulus for 5320-8HS and 5320-PW during their development. However, no significant difference was observed for 5320-8HS and 5320-PW in their plateau values for the manufacturer recommended cure cycle.

Complex Viscosity. Figure 6 shows complex viscosity, η^*, during cure for 5320-8HS and 5320-PW plotted on a semilog scale, for manufacturer recommended cure cycle. The complex viscosity consists of two parts, *viz.* storage modulus and loss modulus. For the two studied prepregs, the behavior of complex viscosity was predominant by its storage modulus. It started dropping initially up to its minimum and then followed by rapid increase indicating the initiation of crosslinking of molecules. Similar to degree of cure and storage modulus, significant difference was observed in complex viscosity for 5320-8HS and 5320-PW during their development for manufacturer recommended cure cycle. However, likewise storage modulus, no significant difference was observed for 5320-8HS and 5320-PW in their plateau values during the applied thermal cycle. It is important to note that both degree of cure and complex viscosity for 5320-PW started deviating from 5320-8HS at the similar time during the curing and the difference between the two started minimizing at the plateau of their complex viscosities.

In addition, no significant change was observed in minimum complex viscosity time for samples cured using different weaves system. This implies that minimum viscosity time is dominated by resin only and the fibers and their interlacing pattern have no significant effect on it.

Damping Factor (tan δ). Gelation represents a change in state from liquid to rubber like state and can be discern with the increase of molecular weight. Generally, gelation does not change the cure rate and hence cannot be determined using DSC. However, the increase in molecular weight significantly changes the viscoelastic properties during cure and can be used to determine gelation.

Figure 7 shows damping factor (tan δ) during cure, obtained using ESR for manufacturer recommended cure cycle for 5320-8HS and 5320-PW. As shown in Figure 7, significant difference was observed in tan(δ) during cure for the two fabric pattern and the values for 5320-PW appeared to be consistently higher

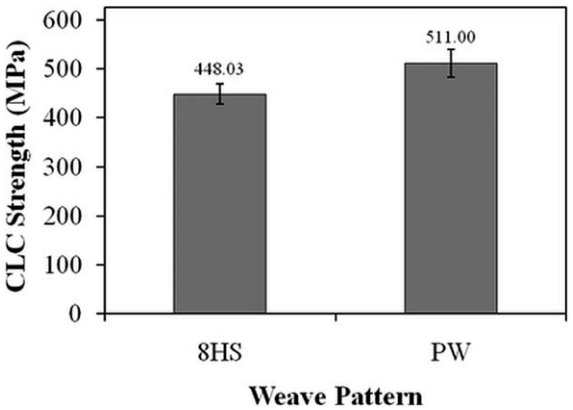

Figure 13. Combined loading compression strength for 5320-8HS and 5320-PW for manufacturer recommended cure cycle.

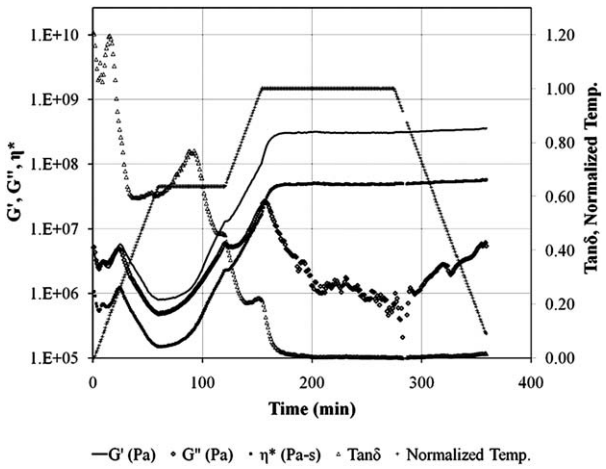

Figure 14. Viscoelastic properties during cure for 5320-8HS for manufacturer recommended cure cycle.

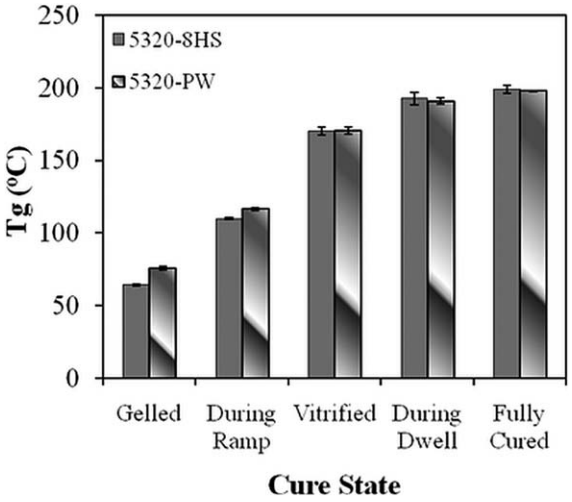

Figure 15. Glass transition temperature development for 5320-8HS and 5320-PW at different cure states during manufacturer recommended cure cycle.

than 5320-8HS during the minimum complex viscosity and gel time.

The sharp drop of tan(δ) was taken as the gel points[22] and is shown in Figure 8. Significant difference was observed in gel time for samples cured using 5320-8HS and 5320-PW. It was observed that the 5320-PW gelled approximately 13 min sooner than 5320-8HS.

Loss Modulus. Vitrification is a transition of cure reactions from kinetic controlled to diffusion controlled mode. Physically, at vitrification the material changes from rubber like state to glassy solid. In literature, vitrification is also defined as the point at which the glass transition temperature of the material equals its curing temperature. After vitrification, the limited mobility of molecules considerably slows down further reactions.[15]

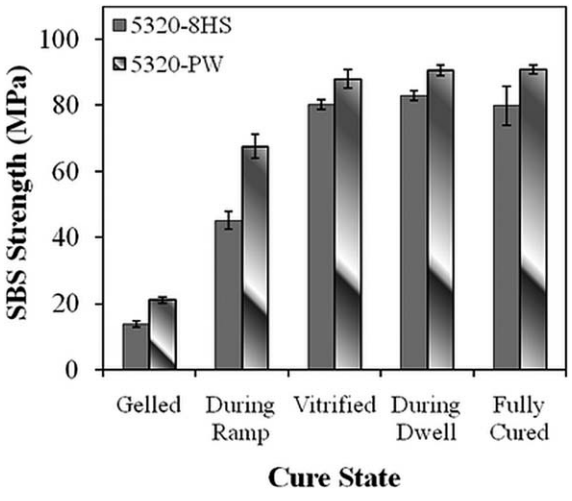

Figure 16. SBS strength comparison between 5320-8HS and 5320-PW for manufacturer recommended cure cycle.

For sufficiently higher heating rates and temperature, the temperature during cure always remains higher than instantaneous glass transition temperature and hence leads to fully cured laminate, i.e., $\alpha = 1$. On the other hand, if the heating rate is slow, at some point during the cure, the glass transition temperature will become equal to the curing temperature leading to the transition of cure reaction from kinetics controlled to diffusion controlled. In the later case, the material will take significant longer time to achieve fully cured state, since the reaction rate is much slower in diffusion controlled reactions than in kinetic controlled reactions.

G'' during cure for 5320-8HS and 5320-PW are shown in Figure 9. The peaks of G'' were used to obtain vitrification time.[22,23] As shown in Figure 10, unlike gel time, no significant difference was observed in the vitrification time for the manufacturer recommended cure cycle for 5320-8HS and 5320-PW.

Glass Transition Temperature. Glass transition temperature of 5320-8HS and 5320-PW samples cured using manufacturer recommended cure cycle were obtained using TA Instruments Q800 dynamic mechanical analyzer (DMA). Figure 11 shows the measured final glass transition temperature (T_g) for 5320-8HS and 5320-PW using DMA. Similar to the final degree of cure obtained using DSC, no significant difference was observed in final T_g values for 5320-8HS and 5320-PW. As such, both DOC and T_g results suggests that they are dependent on each other and can be used to predict the final mechanical properties of the laminate.

Short Beam Shear Properties. Average values for SBS strength of panels cured from 5320-8HS and 5320-PW material using the manufacturer recommended cure cycle along with their respective standard deviation and coefficient of variation are shown in Table II and are plotted in Figure 12.

Table III shows the statistical t test results for short beam shear properties of 5320-8HS and 5320-PW panels, cured using manufacturer recommended cure cycle. It can be seen from the statistical results that, at 95% confidence interval, SBS strength of 5320-PW is higher than 5320-8HS. This is in well agreement with the previous study by Paiva et al. for the same weave but different resin system and can be attributed with the higher inter-laminar resistance offered by the plain weave fabric pattern.[24]

Combined Loading Compression Properties. In contrast to SBS strength values, as shown in Figure 13, CLC strength of 5320-8HS was observed similar to 5320-PW. Table IV shows the statistical t test results for CLC strength for 5320-8HS and 5320-PW panels cured using manufacturer recommended cure cycle. It can be seen from the results that, there is no significant difference in CLC strength of 5320-8HS and 5320-PW panels; since the difference interval varies from negative 1.2 MPa to positive 127.2 MPa and thus includes zero.

Mechanical and Thermal Properties Development During the Cure

In section above, a comparison has been made for viscoelastic and thermal properties between 5320-8HS and 5320-PW for manufacturer recommended cure cycle. In order to investigate

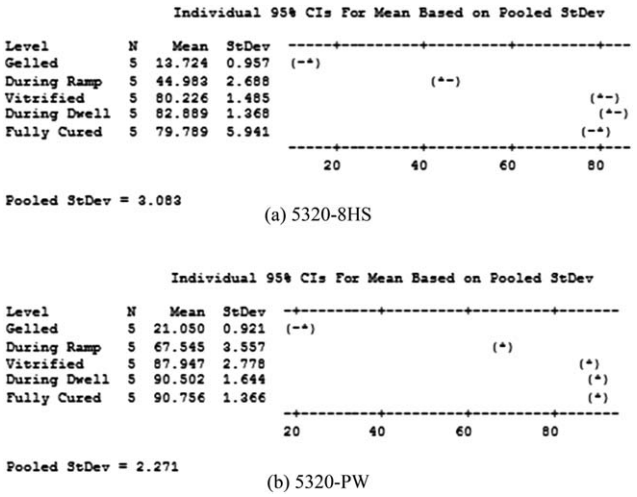

Figure 17. ANOVA analysis of SBS strength at different cure stages.

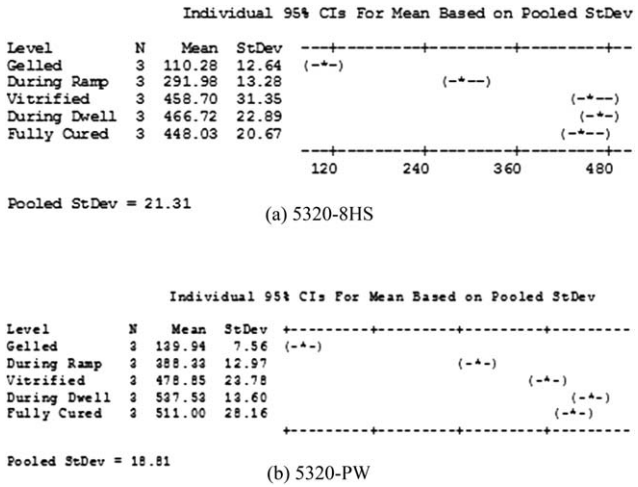

Figure 19. ANOVA analysis of CLC strength at different cure stages.

the mechanical properties development during cure, manufacturer recommended cure cycle was studied at different curing stages for 5320-8HS and 5320-PW. Viscoelastic properties for 5320-8HS obtained using ESR, as shown in Figure 14, were used in designing the cure cycles to study the during cure development of mechanical properties. From the results above, although 5320-PW appeared to become in gel state sooner than 5320-8HS, the same cure cycles were also used for 5320-PW for juxtapose between 5320-8HS and 5320-PW.

Figure 2 and Table I show the cure profiles designed using the viscoelastic definition of the material stages. The during-cure cure cycles were designed carefully to investigate the prepreg properties development during the cure. Important material transitions including gel point and vitrification point were investigated using the designed cure cycles. It is to be noted that gel point was used as a starting point to study the during cure mechanical properties, since the material remains soft before the crosslinking and might had impose machining difficulties. Furthermore, cure cycles were selected based on 5320-8HS since it required more time to achieve gel state, as shown in the results above. Because of the large thermal mass of the panel compared to the ESR sample, an additional time of 10 min of curing was allowed for gel-stage panels to account for the temperature variation inside the oven and to ensure that the material is stiff enough for the machining and specimens preparation.

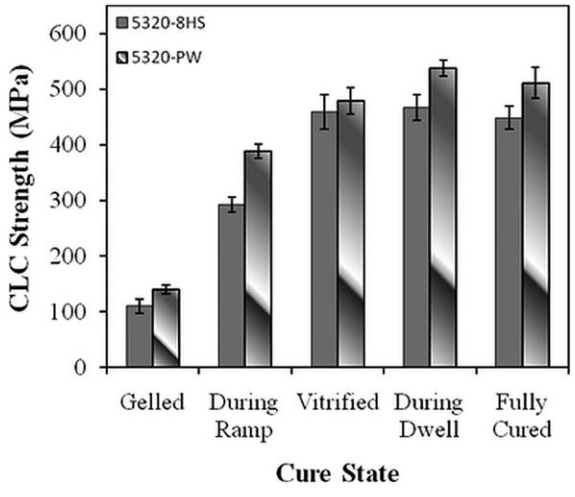

Figure 18. CLC strength comparison between 5320-8HS and 5320-PW for manufacturer recommended cure cycle.

Glass Transition Temperature. To compare and correlate the glass transition temperature with the mechanical properties of the panels, T_g samples of 3 mm × 58 mm long were machined from their respective cured panels and were tested using TA Instruments Q800 dynamic mechanical analyzer (DMA). Figure 15 shows the measured T_g for different cure states for 5320-8HS and 5320-PW obtained using DMA. Similar to the degree of cure development during cure, T_g showed a gradual increase in values with the progress of curing. Moreover, the rate of development of T_g from gel to vitrification was sufficiently higher than the rate after vitrification. This implies that progress of T_g development was also dampened by the diffusion controlled reactions. As such, both DOC and T_g results suggests that they are dependent on each other and can be used interchangeably to predict mechanical properties of the laminate.

Short Beam Shear Properties. Figure 16 presents the comparison of short beam shear strength between 5320-8HS and 5320-PW at different cure stages of manufacturer recommended cure cycle. Similar to fully cured behavior, SBS strength of 5320-PW was observed consistently higher than 5320-8HS during the cure for manufacturer recommended cure cycle. One-way ANOVA analysis, as shown in Figure 17, showed significant difference in SBS strength of 5320-8HS and 5320-PW during cure from gel up to vitrification stage for both the materials. However, no significant development in SBS strength was observed after vitrification for the manufacturer recommended cure cycle.

Combined Loading Compression (CLC) Properties. Average values of CLC strength for 5320-8HS and 5320-PW panels cured using cure cycles mentioned in Table I along with their respective standard deviation are shown in and Figure 18. Similar to SBS development during cure, one-way ANOVA analysis

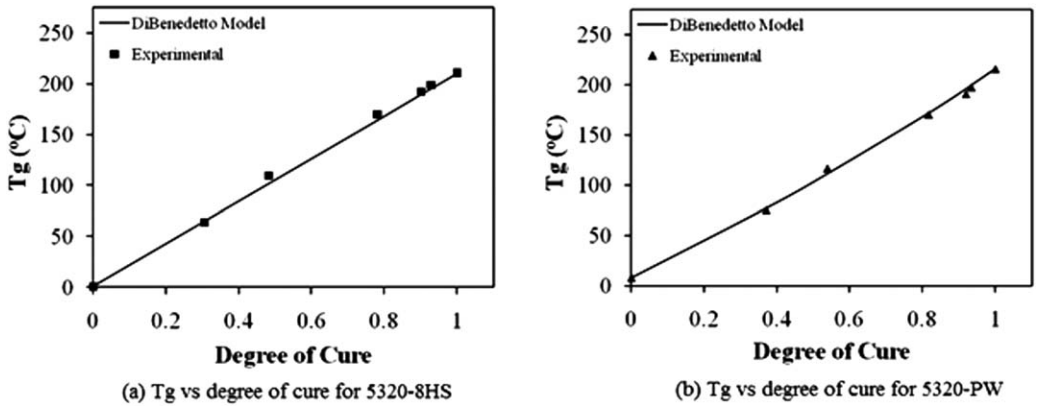

Figure 20. Correlation and Modeling of T_g vs. DOC using DiBenedetto relationship.

of the CLC strength, as shown in Figure 19, showed significant difference in CLC strength during cure from gel up to vitrification stage. However, no significant development in CLC strength was observed after vitrification for the manufacturer recommended cure cycle.

MATHEMATICAL MODELING OF MECHANICAL PROPERTIES

Degree of Cure (DOC) and Glass Transition Temperature (T_g)

As discussed above, both DOC and T_g are important measurements of material cure state. They are strongly dependent on the cure cycle and are directly related to the cure state. In addition, DOC and T_g also have a strong relationship to one another: the higher the DOC, the higher the T_g. Figure 20 shows the DOC plot against T_g obtained using DSC and DMA, respectively, from its gelled state to its fully cured state for 5320-8HS and 5320-PW materials. As the figure shows, T_g of the material gradually increased with the increase in degree of cure for both the materials. Linearly increasing T_g with corresponding increase in DOC suggests that T_g and DOC can be used to substitute each other to represent material cure state.

To validate the observed linear correlation between T_g and DOC, DiBenedetto relation was used. According to Dibendetto relation[25]:

$$T_g = \frac{(1-\alpha)T_{g_0} + \lambda\alpha T_{g_\infty}}{(1-\alpha)+\lambda\alpha} \tag{9}$$

where T_{go} is the subambient glass transition temperature, $T_{g\infty}$ is the ultimate glass transition temperature for the material, λ is the curve fitting parameter.

Table V shows the values of T_{go}, $T_{g\infty}$, and λ obtained for 5320-8HS and 5320-PW. Figure 20 also shows that the predicted model closely matches with the experimental results.

Table V. Modeling Parameters for Correlation Between Material Cure State and Its Physical Properties

Parameter	5320-8HS	5320-PW
T_{go} (°C)	0.8	8.0
$T_{g\infty}$ (°C)	210	216
λ	1.00	0.84
SBS_∞ (MPa)	82.89	90.50
c_1	88.60	215.73
c_2	9.02	11.92
c_3	43.97	65.30
c_4	8.35	9.21

Short Beam Shear (SBS) Strength and Material Cure State

Although DOC and T_g are the most widely used parameters to measure the state of the material, SBS strength can quantify the amount of voids and hence is an important parameter in determining the quality of cured laminate. Therefore, it is highly desirable to obtain composite properties based on DOC, T_g, and SBS properties.

As shown in Figure 21, SBS increased with the increase in degree of cure and glass transition temperature. However, unlike degree of cure and glass transition temperature, the relation was not completely linear. For the initial stage of curing, from b-stage to vitrification, short beam shear strength increased rapidly with the state of cure. However, after vitrification the progress of short beam shear strength development had been dampened by the diffusion controlled reaction. A model was investigated and proposed during this work to predict the SBS strength based on glass transition temperature from its gelled state to its final cured state. The proposed model is as follows:

$$SBS = \frac{SBS_\infty}{\left(1 + c_1 \exp\left(\frac{-c_2 T_g}{T_{g\infty}}\right)\right)} \tag{10}$$

where T_g is the glass transition temperature, $T_{g\infty}$ is the ultimate glass transition temperature, SBS_∞ is the ultimate short beam shear strength, c_1 and c_2 are curve fitting parameters.

To transform the model parameter from glass transition to degree of cure, DiBenedetto relation was used. Equation (11) shows the modified model to predict the SBS strength based on degree of cure of the material.

$$SBS = \frac{SBS_\infty}{\left(1 + c_1 \exp\left(-\frac{c_2}{T_{g\infty}}\left(\frac{(1-\alpha)T_{g_0} + \lambda\alpha T_{g\infty}}{(1-\alpha)+\lambda\alpha}\right)\right)\right)} \tag{11}$$

where α is the degree of cure temperature, T_{go} is the subambient glass transition temperature, $T_{g\infty}$ is the ultimate glass transition temperature of the material, λ is the DiBenedetto model parameter, SBS_∞ is the ultimate short beam shear strength (MPa).

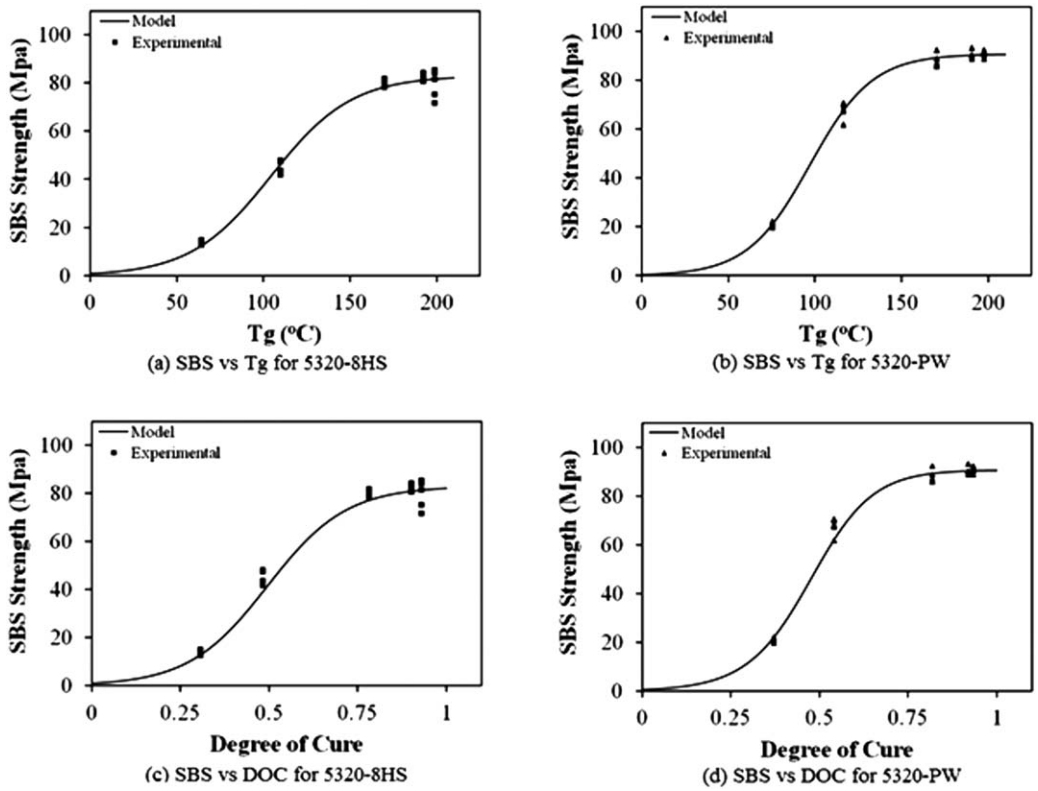

Figure 21. Model plot for short beam shear (SBS) strength.

c_1 and c_2 are curve fitting parameters.

Based on eqs. (10) and (11), curve fitting parameters, c_1 and c_2, were obtained using excel solver and are shown in Table V. The models were subsequently plotted using calculated and experimental parameters and are shown in Figure 21.

Combined Loading Compression (CLC) Strength and Material Cure State

To obtain the relationship between CLC strength and material cure state, first a correlation was obtained by plotting CLC strength against SBS strength as shown in Figure 22 for 5320-8HS and 5320-PW. Good correlation was observed between CLC and SBS strength of 5320-8HS and likewise for 5320-PW.

By taking advantage of observed linear correlation between Combined Loading Compression (CLC) strength and Short Beam Shear (SBS), CLC strength was also plotted based on the similar model as proposed for SBS strength. The models for CLC strength were modified as follows:

$$\mathrm{CLC}=\frac{\mathrm{CLC}_\infty}{\left(1+c_3\exp\left(\frac{-c_4 T_g}{T_{g\infty}}\right)\right)} \tag{12}$$

$$\mathrm{CLC}=\frac{\mathrm{CLC}_\infty}{\left(1+c_3\exp\left(-\frac{c_4}{T_{g\infty}}\left(\frac{(1-\alpha)T_{go}+\lambda\alpha T_{g\infty}}{(1-\alpha)+\lambda\alpha}\right)\right)\right)} \tag{13}$$

where α is the degree of cure temperature, T_{go} and $T_{g\infty}$ are the subambient and ultimate glass transition temperature, respectively. λ is the DiBenedetto model parameter, CLC_∞ is the ultimate combined loading compression strength (MPa), c_3 and c_4 are curve fitting parameters.

Table V shows the modeling parameters used to obtain plots between CLC strength and material cure state. It is worthwhile to note that, although linear relationship was observed between

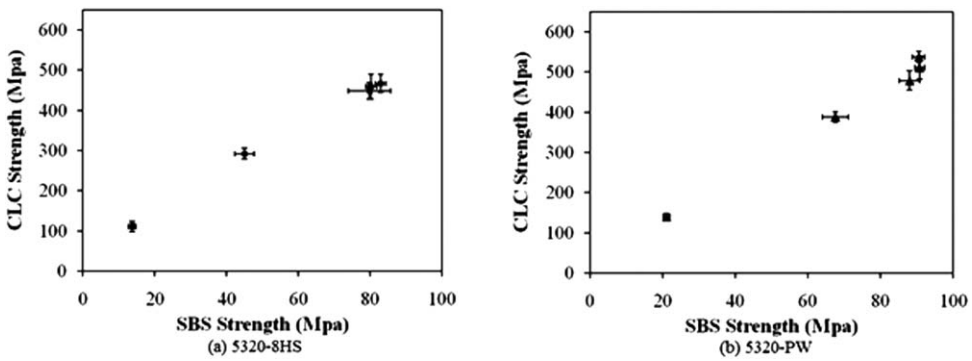

Figure 22. Correlation between CLC and SBS strength.

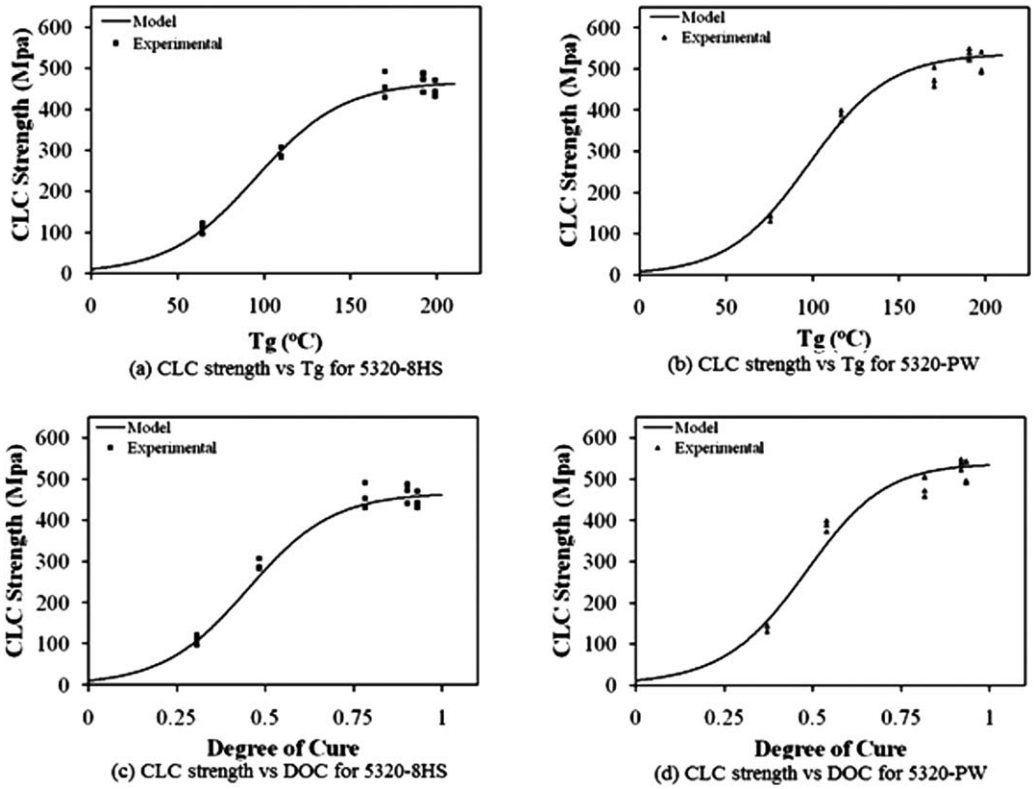

Figure 23. Model plot for combined loading compression (CLC) strength.

SBS and CLC strength, the curve fitting parameters for combined loading compression (CLC) strength models are slightly different than short beam shear (SBS) strength model and can be ascribed as the dispersion of the obtained results within the statistical range. Model plots for combined loading compression (CLC) strength using eqs. (12) and (13) are shown in Figure 23.

CONCLUSIONS

Manufacturer recommended cure cycle was studied for out-of-autoclave materials with two different weave but same resin system. A differential scanning calorimeter (DSC) was used to obtain the degree of cure during applied thermal cycle. Viscoelastic properties during cure were obtained using encapsulated sample rheometer (ESR) while glass transition temperature was obtained using dynamic mechanical analyzer (DMA). Mechanical properties were obtained from the panels at different stages during the cure.

The rate of reaction showed significant effect on the glass transition and hence mechanical properties development during cure. Extensive development of mechanical properties was observed during the manufacturer recommended cure cycle up to vitrification. However, the progress of mechanical properties development was dampened by the diffusion controlled reaction mechanism once the vitrification point was reached.

Significant difference in the properties development was observed between 5320-8HS and 5320-PW material. It was observed that the 5320-PW material reached the gel stage sooner than 5320-8HS. Moreover, statistical results showed that the short beam shear properties of 5320-PW were better than 5320-8HS.

An observed linearly increasing trend between degree of cure (DOC) and glass transition temperature (T_g) for different cure states suggests that both DOC and T_g can be used interchangeably to define the state of material. To further investigate the correlation between state of cure and mechanical properties, degree of cure and T_g both were plotted against short beam shear and combined loading compression strength. A good correlation was observed between material cure state and its SBS and CLC properties. A linear correlation was also observed between SBS and CLC strength. As such, short beam shear strength can be used along with material cure state to predict mechanical properties of the laminate.

To characterize the curing and hence predict the mechanical properties, a model was investigated and proposed for 5320-8HS and 5320-PW. The proposed model can be used to predict the SBS and CLC properties based on either glass transition temperature or degree of cure. Although theoretically all the specimens had the same porosity level, the factor of porosity can easily be accounted for by combining this model with the available models for cylindrical and spherical voids.

REFERENCES

1. Kratz, J.; Hsiao, K.; Fernlund, G.; Hubert, P. *J. Compos. Mater.* **2013**, *47*, 341.

2. Kamal, M. R. *Polym. Eng. Sci.* **1974**, *14*, 231.
3. Chern, C. S.; Poehlein, G. W. *Polym. Eng. Sci.* **1987**, *27*, 788.
4. Hickey, C. M. D.; Bickerton, S. *J. Mater. Sci.* **2013**, *48*, 690.
5. Ruiz, E.; Trochu, F. *J. Compos. Mater.* **2005**, *39*, 881.
6. Lee, W. I.; Loos, A. C.; Springer, G. S. *J. Compos. Mater.* **1982**, *16*, 510.
7. Dusi, M. R.; Lee, W.; Ciriscioli, P. R.; Springer, G. S. *J. Compos. Mater.* **1987**, *21*, 243.
8. Cole, K. C.; Hechler, J. J.; Noel, D. *Macromolecules* **1991**, *24*, 3098.
9. Aronhime, M.; Gillham, J. In Epoxy Resins and Composites III; Dušek, K., Ed.; Springer: Berlin, **1986**; Chapter 3.
10. Kashani, P.; Minaie, B. *J. Reinforced Plast. Compos.* **2011**, *30*, 123.
11. Enns, J. B.; Gillham, J. K. *J. Appl. Polym. Sci.* **1983**, *28*, 2567.
12. Eom, Y.; Boogh, L.; Michaud, V.; Sunderland, P.; Manson, J.-A. *Polym. Eng. Sci.* **2000**, *40*, 1281.
13. Kashani, P.; Alavi-Soltani, S.; Ghods, F.; Minaie, B. In SAMPE Fall Technical Conference, Memphis, **2008**.
14. DeMeuse, M. T.; Gillham, J. K.; Parodi, F. *J. Appl. Polym. Sci.* **1997**, *64*, 15.
15. Cook, W. D.; Scott, T. F.; Quay-Thevenon, S.; Forsythe, J. S. *J. Appl. Polym. Sci.* **2004**, *93*, 1348.
16. Ferry, J. D. Viscoelastic Properties of Polymers; Wiley: New York, **1980**.
17. Riande, E.; Diaz-Calleja, R.; Prolongo, M.; Masegosa, R.; Salom, C. Polymer Viscoelasticity: Stress and Strain in Practice (Plastics Engineering); CRC Press: New York, **1999**.
18. Sabzevari, S. M.; Alavi-Soltani, S.; Minaie, B. *J. Appl. Polym. Sci.* **2011**, *121*, 883.
19. ASTM. In ASTM Standard: D7028-07e1: **2008**.
20. ASTM. In ASTM Standard: D 2344/D 2344M-00: **2000**.
21. ASTM. In ASTM Standard: D 6641/D 6641M-01: **2001**.
22. Alavi-Soltani, S.; Sabzevari, S.; Mousavi, A.; Minaie, B. In International SAMPE Symposium and Exhibition; Baltimore, **2009**.
23. Gernaat, C.; Alavi-Soltani, S.; Guzman, M.; Rodriguez, A.; Minaie, B.; Welch, J. In SAMPE Fall Technical Conference, Wichita, **2009**.
24. Paiva, J. M. F. d.; Santos, A. D. N. d.; Rezende, M. C. *Mater. Res.* **2009**, *12*, 367.
25. DiBenedetto, A. T. *J. Polym. Sci. Part B: Polym. Phys.* **1987**, *25*, 1949.